Three mutations repurpose a plant karrikin receptor to a strigolactone receptor

Amir Arellano-Saab, Michael Bunsick, Hasan Al Galib, Wenda Zhao, Stefan Schuetz, James Michael Bradley, Zhenhua Xu, Claresta Adityani, Asrinus Subha, Hayley Mckay, et al.

Three mutations repurpose a plant karrikin receptor to a strigolactone receptor

Amir Arellano-Saab[1,7], Shigeo Toh[2,7], Hasan Galib[1], Wenda Zhao[1], Stefan Schuetz[1], James Michael Bradley[1], Asrinus Subha[1], Alexandre de Saint Germain[3], Claresta Adityani[1], Michael Bunsick[1], Hayley McKay[1], François-Didier Boyer[4], Christopher S. P. McErlean[5], Peter McCourt[1,8] Peter J. Stogios[6,8] and Shelley Lumba[1,8]

[1] Department of Cell & Systems Biology, University of Toronto, 25 Willcocks Street, Toronto M5S 3B2, Canada

[2] Department of Environmental Bioscience, School of Agriculture, Meijo University
1-501 Shiogamaguchi, Tenpaku-ku, Nagoya, Japan, 468-8502

[3] Institut Jean-Pierre Bourgin, INRAE, AgroParisTech, Université Paris-Saclay, 78000, Versailles, France.

[4] Université Paris-Saclay, CNRS, Institut de Chimie des Substances Naturelles, UPR 2301, 91198, Gif-sur-Yvette, France.

[5] School of Chemistry, The University of Sydney, NSW, 2006, Australia.

[6] Department of Chemical Engineering & Applied Chemistry, Banting & Best Department of Medical Research, University of Toronto, 200 College Street, Toronto M5S 3E5,

[7] Both authors contributed equally to the project

[8] To whom correspondences should be addressed

Uncovering the basis of small molecule hormone receptors evolution is paramount to a complete understanding of how protein structure drives function. In plants, hormone receptors for strigolactones are well suited to evolutionary inquires because closely related homologs have different ligand preferences. More importantly, because of facile plant transgenic systems, receptors can be swapped and quickly assessed functionally *in vivo*. Here, we show only three mutations are required to switch the non-strigolactone receptor, KAI2, into a strigolactone receptor. This modified receptor still perceives KAI2 ligands and does not require receptor hydrolysis for activity. Structural and molecular dynamic modeling suggest receptor pocket flexibility is important for ligand specificity and downstream signaling partner affinity. These findings indicate a few keystone mutations link strigolactone signaling to germination, which explains how parasitic plants that devastate African agriculture evolved SL receptors to sense the presence of a host plant.

Introduction

Plants and animals use small molecule hormones to drive growth and development and for this reason much effort is placed on understanding how hormone receptors perceive their ligands[1,2]. Most inquiries are tuned to identify receptor amino acids that contribute to ligand specificity using "loss-of-function" approaches where an amino acid is replaced with a chemically inert moiety, usually an alanine, and binding is assessed[4,5]. The less explored "gain of function" approach involves swapping amino acids between related receptors that respond to different ligands[6,7]. Gain-of-function approaches have the potential to not only answer questions about receptor-ligand relationships but also can give insights into how receptors evolve. As selection drives changes in the receptor sequence to recognize new ligands, important questions regarding this molecular process can be posed: is this process gradual occurring through many amino acid changes or are only a few keystone substitutions required? When receptors evolve the ability to recognize new ligands, do they lose the ability to bind the ancestral ligands? Gleaning this type of information through gain-of-function approaches, however, has imposing challenges[8]. First, amino acids are not discrete entities acting in isolation but are a sea of interdependent residue. As a result, swapping amino acids into a new context often can result in a non-functional protein due to negative epistasis. Second, depending on the number of potential swaps, the number of

variants can quickly scale limiting analysis to simple *in vitro* assays rather than more complex *in vivo* analysis.

With this said, the perception of the plant hormone strigolactone (SL) may be a useful system to understanding the evolution of small molecule receptors. The root parasite *Striga hermonthica* (*Striga*), for example, uses a group of α/β hydrolases designated HYPOSENSITIVE TO LIGHT (ShHTL) to perceive host-derived SLs allowing the parasite to coordinate its germination with the lifecycle of a host plant[9]. By contrast, the homologous protein, HYPOSENSITIVE TO LIGHT/KARRIKIN INSENSITIVE 2 (KAI2), which is also involved in germination in the model plant *Arabidopsis thaliana* (*Arabidopsis*), is not considered an SL receptor[10,11]. Plants only produce SLs with a 2'*R* enantiomeric configuration in D-ring but this enantiomer is not recognized by KAI2 (**Supplementary Fig. 1**)[12,13]. In *Arabidopsis*, (2'*R*)-SLs are recognized by a more distantly related α/β hydrolase, DWARF14 (AtD14), a receptor that is only involved in vegetative growth[14,15]. Instead KAI2 responds to a collection of smoke-derived butenolides collectively called karrikins (KARs)[16], and strangely is activated by non-natural (2'*S)*-SL enantiomers (**Supplementary Fig. 1**)[13]. This has led to suggestions that KAI2, like ShHTL receptors, positively regulates germination not by using naturally occurring (2'*R*)-SLs but by perceiving an unidentified butenolide-based ligand, designated KAI2-ligand (KL)[17]. Because parasitic lifestyles are derived from nonparasites, this implies that ShHTL parasitic receptors evolved the ability to perceive (2'*R*)-SLs from ancestor KAI2 receptors that bind KL[18].

Structural analysis of KL and SL receptors generally conclude that ShHTL receptors have larger binding sites with a broader set of active site amino acids allowing for greater responsiveness to an array of (2'*R*)-SL molecules, a trait thought to increase *Striga* host range[19]. There are also suggestions that receptor affinity to downstream signaling partners also contributes to ligand responsiveness[20]. The separation of ligand specificity versus partner affinity helps to resolve the conundrum of how *Striga* SL receptors show decreased specificity but increased sensitivity to the same ligand. These conclusions, however, are based solely on *in vitro* experiments because *Striga* is an experimentally intractable genetic system[21]. Fortunately, ShHTL receptors function in *Arabidopsis* mutants deficient in KAI2 function and under specific conditions confers seed germination sensitivity to SLs[11,22]. Furthermore, model plants like *Arabidopsis*, unlike their animal counterparts, are easily transformed[23] making high throughput analysis at the whole organism level feasible. This cross-species functionality means

homologous-substitution mutagenesis between KL-based KAI2 and SL-based ShHTL receptors can be performed to probe evolutionary questions of ligand sensitivity, specificity and promiscuity in an *in vivo* context.

With this in mind, here we systematically substituted key amino acids from the highly responsive ShHTL7 SL receptor at homologous positions in KAI2 and assayed their ability to sense SLs *in vivo*. We show using both yeast- and plant-based assays, that only three amino acid changes were required to repurpose KAI2 into an SL receptor that recognizes (2'*R*)-SL enantiomers. The emergent properties of this chimeric KAI2 receptor does not appear to require loss of KL perception. Furthermore, ligand perception does not require receptor hydrolysis. Structural and molecular dynamic modeling indicates substitution of three active site amino acids from ShHTL7 into KAI2 produces a larger more flexible binding pocket that better accommodates SLs including (2'*R*)-SL enantiomers and most likely allows better interactions with downstream signaling partners. The relatively simple mutational path to convert KAI2 into a SL receptor together with the central role of KAI2 in non-parasitic plant germination has implications with respect to the molecular mechanism of how *Striga* co-opted this regulator to be a germination sensor of host-derived SLs.

Results

Identifying amino acids involved in SL binding. KAI2 and ShHTL receptors share β-sheet cores flanked by α-helices with their ligand binding pockets covered by a V-shaped cap[24-27]. Within the binding pocket is a catalytic triad of amino acids that is involved in ligand hydrolysis[9,27-29]. To identify important amino acid differences between a KL and an SL receptor we compared amino acid sequences within the ligand binding pocket of KAI2 to the *Striga* SL receptor, ShHTL7, which both have experimental 3D structures available[11,22]. Because the larger ShHTL7 binding pocket can accommodate (2'*R*)-SLs[19,20], we focused on ShHTL7 residues that were less bulky and/or more polar than their homologous counterparts in KAI2 (**Supplementary Fig. 2**). This identified eight ShHTL7 amino acids (Leu26, Tyr124, Thr142, Leu153, Thr157, Tyr174, Thr190, Cys194) that we substituted into the equivalent homologous position in KAI2 in all single, double and triple combinations to generate 92 chimeric KAI2 gene variants.

Three substitutions change KAI2 responsiveness to SL. To systematically test the 92 chimeric KAI2 receptors, we developed two *in vivo* high throughput SL receptor responsive assays. KAI2 interacts with its signaling partner MORE AXILLARY MERISTEMS 2 (MAX2)[30] making this interaction a good candidate for a yeast two-hybrid assay (Y2H). KAI2, however, autoactivates in Y2H assays in some conditions[31] and MAX2 is also unstable in yeast[19]. Therefore, we developed Y2H growth conditions where KAI2 did not autoactivate (**see Supplementary Materials & Methods**) and fragmented MAX2 into nine constructs (N1-N9) to identify a fragment that produced a positive Y2H signal in the presence of a SL (**Supplementary Fig. 3**). Although KAI2 (Var1) and the chimeric receptor variants (Var2-Var93) showed no or poor interactions with most MAX2 fragments, the N3 fragment interacted with some chimeric receptors to varying degrees, in the presence of a racemic mixture (2'*R,* 2'*S*) of the artificial SL, *rac*-GR24 (**Fig 1a**). With a cut off of four standard deviations above the mean interaction intensity this experiment identified seven variants (Var21, 37, 62, 64, 65, 66, 67) that showed *rac*-GR24-dependent N3 interactions (**Fig. 1b**). Six of these variants contained a ShHTL7 amino acid substitution at position 190 and four variants contained substitutions in positions 124 or 157 suggesting that these amino acids influence the *rac*-GR24-dependent interactions in yeast (**Supplementary Fig. 3**). The identification of amino acids positioned at 124, 157 and 190 is consistent with *in vitro* studies that show these amino acids are important for SL binding[19,20].

Parallel to our Y2H assays, we evaluated all 92 of the chimeric KAI2 receptors by transforming them into *Arabidopsis* deficient for KAI2 function (*htl-3*)[30]. Using an SL-dependent germination assay involving GA-depleted seeds[11], we found the one line, Var64 (Trp153Leu, Phe157Thr, Gly190Thr), germinated well upon *rac*-GR24 addition (**Fig. 1a).** Subsequent analysis of three independent transgenic lines (64A, 64B, 64C) showed 50 percent germination (EC_{50}) at high nanomolar concentrations of $GR24_{rac}$ (**Fig. 1c**). Interestingly, Var19 lines (Trp153Leu, Gly190Thr), which contains a subset of Var64 amino acids, showed the next highest level of *rac*-GR24-dependent germination in our *in planta* assay (**Fig. 1a**, **Supplementary Fig. 4**). Notably, the Var64 receptor variant was also identified in our Y2H assay, indicating that two independent assays showed that substitution of Leu153, Thr157 and Thr190 into KAI2 greatly improved its responsiveness to *rac*-GR24.

The identification of Leu153, Thr157 and Thr190 as having roles in SL perception encouraged us to determine the prevalence of these amino acids in KAI2-related proteins across

a large collection of land plants. Focusing on clades of receptors that are not expected to bind SLs (conserved) versus clades of receptors that are expected to bind SLs (divergent)[18] we found conserved clades were mostly devoid of ShHTL7-related amino acids whilst the divergent clades were highly populated with ShHTL7-related residues (**Fig. 2**). Divergent KAI2 proteins were particularly enriched for 153Leu or hydrophobic amino acids at this position, and proteins more closely related to ShHTL7 possessed similar amino acids at positions 157Thr and 190Thr (**Fig. 2**). Interestingly, within the divergent group, the one clade of proteins depleted of ShHTL7 amino acid identities were most closely related to receptors ShHTL10 and ShHTL11 (e.g. *SaKAI2d2, 10, 11, 16, ShKAI2d10, 11*) which do not have a role in germination as assayed by *Arabidopsis*[22]. Together, the distribution of ShHTL7 amino acids across land plants suggests that our *in vivo* screening identifies important amino acids involved in the evolutionary switch of KAI2 to an SL receptor. Finally, the observation that both our assays led to the Var64 amino acid combination suggests that the simpler and less time consuming yeast-based protein interaction assays may be a good first screen before plant-based assays.

KAI2 variant 64 recognizes natural occurring (2'*R)*-SL. The SL responsiveness of Var64 seed may be due to increased sensitivity to either or both enantiomers of $GR24_{rac}$. To differentiate between these possibilities, we measured the germination response of three independent Var64 lines (64A, 64B, 64C) to either (2'*S*)- or (2'*R*)-GR24 in our GA-depletion assay[11]. Compared to misexpressed KAI2, the Var64 lines showed more sensitivity to *2'S*-GR24 but importantly showed responsiveness to (2'*R*)-GR24, a property not present in the wild type KAI2 receptor (**Fig. 3a**). We also noticed that compared to KAI2 seed, Var64 lines germinated at low levels, even in the absence of *rac*-$GR24_{rac}$, suggesting a weakly constitutive germination phenotype in the absence of SL addition (**Fig. 3a**). Suppressor analysis in rice identify GID1 α/β hydrolase GA receptor mutants with weak GA constitutive phenotypes that are enhanced by GA addition[32]. This is thought to be due to alterations in the conformation of the receptor's lid subdomain that increases its affinity for interactions with its downstream signaling partners[32]. By analogy, ShHTL7 amino acids may alter the active site of KAI2 to a conformation closer to the "on state", which may improve downstream protein interactions. Consistent with this, the positions 153 and 157 are important in MAX2 and SMAX1 interactions with ShHTL7 *in vitro*[20].

To biochemically characterize the molecular mechanism of Var64 signalling, we first measured hydrolysis activity of Var64 variant receptors using the YLG assay[9]. Var64 receptors showed weak YLG hydrolysis activity compared to WT KAI2 enzyme, but this activity was inhibited by addition of *rac*-$GR24_{rac}$, indicating that SL indeed bind the variant receptor (**Fig. 3b**). To more directly measure SL hydrolysis we monitored D-ring production by HPLC from hydrolysis of either (−)-(2'*S*)- or (+)-(2'*R*)-GR24 and again found neither GR24 enantiomer was a substrate compared to KAI2, which has a preference for (2'*S*)-SLs, or ShHTL7, which has a preference for (2'*R*)-SLs (**Fig. 3c**). In summary, although Var64 seed showed improved germination on (2'*S*)-GR24 and an emergent ability to germinate on the (2'*R*)-GR24 the Var64 protein at best, has poor hydrolysis activity for these two enantiomers. This suggests this receptor variant functions in response to SL *in vivo* but with minimal hydrolase activity.

KAI2 variant 64 responds to karrikins. Because the identity of KL is unknown, we cannot directly assess its binding to our variant receptors. However, KL also has a role in *Arabidopsis* leaf development[33], which means rescue of the *htl-3* leaf mutant phenotype by variant receptors in transgenic plants can be used as a readout of endogenous KL binding to its receptor. Under our growth conditions, *htl-3* leaf length to width ratios are smaller (≤1.85) versus wild type leaves (≥1.92) and this difference can be used to quantify the degree to which chimeric variants can complement *htl-3* leaf shape defects (**Supplementary Fig. 5**). Generally, higher order mutant lines showed less rescue of *htl-3* leaf mutant phenotype than lower order mutants, which could reflect a loss of endogenous KL recognition (**Fig. 1a**). This pattern, however, may also be due to increasing negative epistasis as newly introduced amino acids pile up resulting in non-functional proteins[8]. We noticed, however, that triple substitution variant lines that carried a ShHTL7 amino acid at position 190 complemented *htl-3* leaf defects more often than other triple mutant or even double mutants lacking this substitution (**Fig. 1a**). Deep sequencing analysis suggest that amino acid substitutions can be neither positive nor negative in terms of protein function, but simply stabilize proteins and allow for a larger number of substitutions to be tolerated during evolution[34]. Perhaps, Threonine at position 190 is a permissive substitution that opens alternative mutational paths for ligand recognition. With this said, Var64 lines, which contain a Thr190 substitution, complemented *htl-3* leaf defects suggesting that this chimeric receptor retained an ability to recognize KL (**Fig. 1a**). Although this cannot be directly tested,

Var64 seed germinated on KAR_2 to a similar level seen for KAI2 seed, indicating that this chimeric variant retains the capacity to recognize a native KAI2 ligand.

KAI2 variant 64 protein-ligand dynamics. Structural comparisons of the Var64 protein model to a wild type KAI2 crystallographic structure (PDB 4IH1[xx]) showed that replacing KAI2 aromatic residues Trp153 and Phe157 with Leu and Thr, disrupted several hydrogen bond interactions that would occur between the αB, αC, and αD helices of the lid domain (**Fig. 4a, b**). This change would increase the pocket mouth area from 45.5 $Å^2$ to 57 $Å^2$, which would allow for larger substrates, such as GR24, to access the active site of the receptor more easily. These disruptions would also result in the increase of the overall pocket solvent-accessible volume by approximately 140 $Å^3$ (**Fig. 4a, b**). Larger binding pockets should increase ligand accessibility but to explore this in more detail we modeled (2'*R*)-GR24 ligand-receptor interactions using molecular dynamics (MD) simulations. Unlike traditional structural docking analysis, which is a static snapshot of the protein structure, MD simulations take into account the temporal evolution and velocities of all of the atoms of a protein averaged over a specific period of time to give a more realistic atomic-level detail of the protein. MD simulations of Var64 and KAI2 receptors in the presence of (2'*R*)-GR24, as well as their apo states, were conducted in triplicate 10 ns simulations to evaluate the dynamics of these ligand-receptor complexes in contrast with the unbound receptor, calculating the number and distance of hydrogen bonds that form between receptor and ligand, and measuring the fluctuation of the ligand positions throughout the simulation. To quantitatively distinguish between ligand binding states, we defined productive modes to include states in which (2'*R*)-GR24 was close to the receptor (≤5.0 Å) and its surface area was mostly covered by the active site of the protein. The unproductive mode incorporates instances where the ligand was further away from the pocket opening (5.1-7.0 Å) and not interacting with the active site. Finally, a dissociated mode comprised states where (2'*R*)-GR24 was far from the protein (≥7.5 Å) thus any interactions are very unlikely. Using these criteria, (2'*R*)-GR24 was in a productive binding mode with the Var64 receptor almost 50% of the simulation time versus only 2.1% for KAI2 (**Fig. 4c**). Furthermore, when docked on KAI2, (2'*R*)-GR24 spent approximately 65% of the simulation time in a dissociated mode versus 10% for Var64. Finally, we calculated the magnitude of location change of the position of (2'*R*)-GR24 on the two receptors. For a productive ligand-receptor interaction, a minimal fluctuation is

expected, as the ligand is tightly bound until it is metabolized or released. The simulations showed that the position of (2'*R*)-GR24 in KAI2 fluctuates between 0.02 and 0.18 nm once initially bound to the protein, by contrast, this oscillation is greatly reduced in the Var64 protein, confirming the ability of the new variant to form a stable interaction with an SL ligand (**Fig. 4d**).

Visualization of the trajectory of the MD simulations revealed that the motility of the αE loop of unbound Var64 is increased, consistent with our model of increased flexibility of the receptor's active site and the expansion of the cavity depth and volume (**Supplementary Movie 1**). The trajectories also show three main changes between bound and unbound receptors. First, the hydrophobicity of the binding domain of Var64 was slightly reduced throughout the simulation after binding of (2'*R*)-GR24, which is qualified by the change in coloration from orange to blue in the binding domain region. Second, (2'*R*)-GR24 appears to be more attracted by the polar ShHTL7 Thr190 in Var64 than the KAI2 Gly190. Possibly, this substitution is the reason for the higher ligand stability provided by Var64. Lastly, we observe a conformational change of the αD helix of Var64 upon binding to (2'*R*)-GR24 (**Supplementary Movie 2**). This conformational change is expected in the SL perception pathway, as SL bound receptors have been shown to adapt the conformation of the αD helix to accommodate interactions with its downstream partners[20,35,36].

Discussion

Structurally guided mutational analysis is an effective approach to dissecting how a protein's sequence contributes to biochemical activity, but how these biochemical properties evolve is more experimentally challenging[8]. From an evolutionary perspective, loss-of-function approaches are not necessarily informative and often experiments on protein evolution are not performed in an *in vivo* context which allows proteins to interact with other cellular constituents and processes. In this study, we used a gain-of-function approach with active site amino acid targeted substitutions informed by structural and evolutionary considerations to determine if a non-parasitic plant orphan receptor, KAI2, that is incapable of recognizing natural SL ligands harnessed by parasitic plants, could be converted into a receptor that recognizes such ligands. Importantly, we assayed these receptor variants using yeast- and *Arabidopsis*-based systems to evaluate receptor function under *in vivo* conditions.

Our approach unambiguously determined that only three amino acid substitutions were necessary to convert KAI2 into a functional SL receptor. By introducing smaller, more polar amino acids into KAI2, we produced a protein with a more flexible pocket and lid; this affects receptor function in two ways. First, it increases the pocket volume to accommodate natural SL conformations like that of (2*R'*)-GR24. Second, it increases the overall elasticity of the protein, which may allow better interactions with signaling partners[20,35,36]. To this end, the identification of positions 153, 157 and 190 in our *in vivo* experiments is consistent with the *in vitro* conclusions about these amino acids[19,20]. Our *in vivo* findings contribute to discussions concerning the role of gradual versus keystone mutations in small molecule receptor evolution. Animal studies using ancestral gene reconstructions involving steroid receptors show as few as two mutations can switch ligand specificity[37]. Our results now extend the importance of keystone mutations to plant hormone receptor evolution.

General models of hormone evolution suggest promiscuous ancestral forms evolve specificity so as to prevent deleterious ligand crosstalk[38]. Three lines of evidence in this study, however, suggest a path to SL perception in KAI2 does not necessarily require loss of responsiveness to previous ligands. First, our variant receptor complements the KAI2 loss-of-function phenotype suggesting it still recognizes the endogenous KAI2 ligand. Second, variant receptor seeds are sensitive to (2'*S*)-GR24 enantiomers, a known substrate for KAI2. Finally, variant lines respond to the KAI2-specific exogenous ligands, karrikins. The ability of variant receptors to respond to both ancestral as well as derived ligands supports the notion that SL perception can evolve through sufficient promiscuity rather than by a narrowing of specificity. The sufficient promiscuity models receptor specificity as being adequate but not overly so to distinguish endogenous ligands[39]. This "just enough" specificity explains why receptors often show sensitivity to drug structures unrelated to their natural ligands. The discovery of an artificial femtomolar responsive ShHTL7 agonist with little similarity to SLs further supports a sufficient promiscuity model for these receptors[40].

It also appears that the tight connection between SL hydrolysis and SL perception is not necessary as Var64 variant seed responded to GR24 enantiomers as the Var64 protein showed little hydrolase activity. The role of ligand hydrolysis in SL signaling is somewhat contentious with structural studies producing conflicting models[41,42]. Chemical biology suggests hydrolysis is important to signaling sensitivity but again may not be essential[30,40]. Finally, mutational analysis

of the D14 receptor in *Arabidopsis* indicates hydrolysis is both necessary[29] and not necessary[42] for SL signaling. Although our results support a less direct connection between of hydrolysis and signaling, our variant receptor most likely does not reflect the natural progression by which KAI2 genes evolved to become SL receptors in *Striga*. Our KAI2 variants were not under the constant constraints seen in natural environments that are important for fitness. This may explain why in contrast to the yeast-based interaction assay, we only found one variant with high SL responsiveness *in planta*. We understand that monitoring KAI2 function using the output of *Arabidopsis* germination is superior to *in vitro* based experiments but even this system almost certainly overestimates the frequency of beneficial mutations relative to natural evolution. With this said, the correlation of ShHTL7 153, 157 and 190 amino acids in divergent versus conserved KAI2 is consistent with these residues playing key roles in SL perception. Finally, directed protein engineering studies tell us that enzymes usually possess minor non-selective activities that are often enhanced by laboratory evolution[44,45]. If true, KAI2 may possess a to-date undetected low level of responsiveness to 2'*R* enantiomers. *In vitro*, KAI2 only appears to bind (2'*S*)-GR24[29] but *in vivo,* KAI2 can perceive (2'*R*)-GR24 but only when the SL receptor, D14, is defective[46], suggesting that the absence of D14 uncovers the latent binding ability of KAI2 for 2'*R* enantiomers as it would be free from competition for (2'*R*)-SL substrates with endogenous D14.

The role of KAI2 in germination together with its ability to perceive small molecules makes it easy to understand why this gene was co-opted during the evolution of *Striga* parasitism. *Striga* plants not only requires a host for growth but also requires a cue to signal the proximity to a host, and a long-term survival strategy in the absence of a host. Since SLs are needed for beneficial plant root-AM fungi interactions[47], secretion of these small molecules makes it an excellent plant root positional cue. Seeds are an attractive solution to establishing long-term viability in the absence of a host as dormant seeds can survive long periods under a variety of environmental conditions. An unintended agricultural consequence of using dormant seeds as the protective state in the absence of a host is that they easily contaminate soil and are difficult to purge from farmers fields. For these reasons, *Striga* has contaminated over 20 African nations and is the largest biological impediment to food security on the continent[48,49]. Understanding the steps by which KAI2 evolved to become a SL receptor will give insights not only into the role of this key regulator of the *Striga* lifecycle but will also help define the

335 chemical space of this receptor, which should open leads to new chemical solutions to this
336 African scourge.

Reference

1. Evans, R. M. & Mangelsdorf, D. J. Nuclear Receptors, RXR, and the Big Bang. *Cell*, **157**, 255–266 (2014).
2. Lumba, S., Cutler, S. & McCourt, P. Plant nuclear hormone receptors: a role for small molecules in protein-protein interactions. *Annu Rev Cell Dev Biol*. **26**, 445-469 (2010).
3. Morrison ,K. L. & Weiss, G. A. Combinatorial alanine-scanning. *Curr Opin Chem Biol*. **5**, 302-307 (2001).
4. Howlader, M.T. et al. Alanine scanning analyses of the three major loops in domain II of *Bacillus thuringiensis* mosquitocidal toxin Cry4Aa. *Appl Environ Microbiol*. **76**, 860-865 (2010).
5. Zhao, L., et al. Destabilization of strigolactone receptor DWARF14 by binding of ligand and E3-ligase signaling effector DWARF3. *Cell Res* **25**, 1219–1236 (2015).
6. Kobilka, B.K., et al. Chimeric alpha 2-,beta 2-adrenergic receptors: delineation of domains involved in effector coupling and ligand binding specificity. *Science* **240**, 1310–16 (1988).
7. Cunningham, B. C., Jhurani, P., Ng, P. & Wells, J. A. Receptor and antibody epitopes in human growth hormone identified by homolog-scanning mutagenesis. *Science* **243**, 1330–36 (1989).
8. Hochberg, G. K. A. & Thornton, J. W. Reconstructing Ancient Proteins to Understand the Causes of Structure and Function. *Annu Rev Biophys*. **46**, 247-269 (2017).
9. Tsuchiya, Y., et al. PARASITIC PLANTS. Probing strigolactone receptors in *Striga hermonthica* with fluorescence. *Science*. **349**, 864-868 (2015).
10. Scaffidi, A., et al. Strigolactone Hormones and Their Stereoisomers Signal through Two Related Receptor Proteins to Induce Different Physiological Responses in Arabidopsis. *Plant Physiol*. **165**, 1221-1232 (2014).
11. Bunsick M, et al. SMAX1-dependent seed germination bypasses GA signalling in *Arabidopsis* and *Striga*. *Nat Plants*. **6**, 646-652 (2020).
12. Yoneyama, K., Xie, X., Yoneyama, K., et al. Which are the major players, canonical or non-canonical strigolactones? *J Exp Bot*. **69**, 2231-2239 (2018).
13. Flematti, G. R., Scaffidi, A., Waters, M. T. & Smith, S. M. Stereospecificity in strigolactone biosynthesis and perception. *Planta*. **243**,1361-1373 (2016).

14. Brewer, P. B., Koltai, H. & Beveridge C. A. Diverse roles of strigolactones in plant development. *Mol Plant*. **6**, 18-28 (2013).
15. Waldie, T., McCulloch, H. & Leyser, O. Strigolactones and the control of plant development: lessons from shoot branching. *Plant J*. **79**, 607-622 (2014).
16. Flematti, G. R., Ghisalberti, E. L., Dixon, K. W. & Trengove, R. D. A compound from smoke that promotes seed germination. *Science* **305**, 977 (2004).
17. Conn, C. E. & Nelson, D. C. Evidence that KARRIKIN-INSENSITIVE2 (KAI2) Receptors may Perceive an Unknown Signal that is not Karrikin or Strigolactone. *Front Plant Sci*. **6**, 1219 (2016).
18. Conn, C.E., et al. PLANT EVOLUTION. Convergent evolution of strigolactone perception enabled host detection in parasitic plants. *Science*. **349**, 540-543 (2015).
19. Xu, Y., et al. (2018). Structural analysis of HTL and D14 proteins reveals the basis for ligand selectivity in *Striga*. *Nat Commun*. **9**, 3947 (2018).
20. Wang et al., *Plant Physiol*. 2020 in press
21. Spallek, T., Mutuku, M. & Shirasu K. The genus *Striga*: a witch profile. *Mol Plant Pathol*. **14**, 861-869 (2013).
22. Toh, S., et al. Structure-function analysis identifies highly sensitive strigolactone receptors in *Striga*. *Science*. **350**, 203-207 (2015).
23. Clough, S. J. & Bent, A. F. Floral dip: a simplified method for Agrobacterium-mediated transformation of *Arabidopsis thaliana*. *Plant J*. 16, 735-743 (1998).
24. Kagiyama, M., et al. Structures of D14 and D14L in the strigolactone and karrikin signaling pathways. *Genes Cells*. **18**, 147-160 (2013).
25. Guo Y., et al Smoke-derived karrikin perception by the α/β-hydrolase KAI2 from *Arabidopsis*. *Proc Natl Acad Sci U S A*. **110**, 8284-8289. (2013).
26. Shahul Hameed, U., et al. Structural basis for specific inhibition of the highly sensitive ShHTL7 receptor. *EMBO Rep*. **19**, e45619 (2018).
27. Hamiaux, C., et al. DAD2 is an α/β hydrolase likely to be involved in the perception of the plant branching hormone, strigolactone. *Curr Biol*. **22**, 2032–2036. (2012).
28. de Saint Germain, A., et al. An histidine covalent receptor and butenolide complex mediates strigolactone perception. *Nat Chem Biol*. **12**, 787–794 (2016).

29. Waters, M. T., Scaffidi, A., Flematti, G., & Smith, S. M. Substrate- induced degradation of the α/β-fold hydrolase KARRIKIN INSENSITIVE2 requires a functional catalytic triad but is independent of MAX2. *Mol Plan*t. **8**, 814–817 (2015).
30. Toh S, et al. (2014). Detection of Parasitic Plant Suicide Germination Compounds Using a High-Throughput *Arabidopsis* HTL/KAI2 Strigolactone Perception System. *Chem Biol*. **2**, 988-998 (2014).
31. Yao, J., et al. An allelic series at the KARRIKIN INSENSITIVE 2 locus of *Arabidopsis thaliana* decouples ligand hydrolysis and receptor degradation from downstream signalling. *Plant J.* **96**, 75-89 (2018).
32. Yamamoto, Y. et al. A rice *gid1* suppressor mutant reveals that gibberellin is not always required for interaction between its receptor, GID1, and DELLA proteins. *Plant Cell*. **22**, 3589-3602 (2010).
33. Waters, M. T., et al. Specialisation within the DWARF14 protein family confers distinct responses to karrikins and strigolactones in *Arabidopsis*. *Development*. **139**, 1285-1295 (2012).
34. Starr, T. N. & Thornton, J. W. Epistasis in protein evolution. *Protein Sci*. **25**, 1204-1218 (2016).
35. Bürger, M., et al. Structural Basis of Karrikin and Non-natural Strigolactone Perception in *Physcomitrella patens*. *Cell Rep*. **26**, 855-865 (2019).
36. Lee, H. W., et al. Flexibility of the petunia strigolactone receptor DAD2 promotes its interaction with signaling partners. *J Biol Chem*. **295**, 4181-4193 (2020).
37. Harms, M. J., et al. Biophysical mechanisms for large-effect mutations in the evolution of steroid hormone receptors. *Proc Natl Acad Sci U S A*. **110**, 11475-11480 (2013).
38. Tawfik, D. S. Messy biology and the origins of evolutionary innovations. *Nat Chem Biol* **6**, 692–696 (2010).
39. Eick, G. N., et al. Evolution of minimal specificity and promiscuity in steroid hormone receptors. *PLoS Genet*. **8**, e1003072 (2012).
40. Uraguchi, D., et al. (2018). A femtomolar-range suicide germination stimulant for the parasitic plant *Striga hermonthica*. *Science*. **362**, 1301-1305 (2018).
41. Yao, R., et al. (2016). DWARF14 is a non-canonical hormone receptor for strigolactone. *Nature* **536**, 469–473 (2016).

42. Shabek, N., et al. Structural plasticity of D3-D14 ubiquitin ligase in strigolactone signalling. *Nature*. **563**, 652-656 (2018).
43. Seto, Y., et al. Strigolactone perception and deactivation by a hydrolase receptor DWARF14. *Nat Commun*. **10**, 191 (2019).
44. Bloom JD, Arnold FH (2009) In the light of directed evolution: pathways of adaptive protein evolution. *Proc Natl Acad Sci U S A* **106** Suppl 1, 9995–10000.
45. Khersonsky O, Tawfik DS (2010) Enzyme promiscuity: a mechanistic and evolutionary perspective. *Annu Rev Biochem* **79**, 471–505.
46. Villaecija-Aguilar, J. A., et al. (2019) SMAX1/SMXL2 regulate root and root hair development downstream of KAI2-mediated signalling in *Arabidopsis*. PLoS Genetics, 15 (8) (2019).
47. Akiyama, K., Matsuzaki, K. & Hayashi, H. Plant sesquiterpenes induce hyphal branching in arbuscular mycorrhizal fungi. *Nature*. **435**, 824-827 (2005).
48. Ejeta, G. (2007) The *Striga* scourge in Africa: A growing pandemic. Integrating New Technologies for *Striga* Control, pp. 3-16
49. Parker, C. Observations on the current status of *Orobanche* and *Striga* problems worldwide. *Pest Manag. Sci.* **65**, 453–459 (2009).

Figure 1. Identification of a variant KAI2 that perceives SL. a. Heatmap representation of SL-dependence of the 93 KAI2 chimeric variants. Var1 is the KAI2 wild type control. Lanes 1-2; Yeast two hybrid assays where increased purple shading represent an increased interaction intensity on *rac*-GR24 relative to the DMSO control for KAI2 chimeric variants queried against the N3 MAX2 fragments (**Supplementary Fig. 3**). Interaction strengths were quantified using colony color intensity after 72 hours. Representative colonies for Var27 and Var64 are shown on the left inserts. Lanes 3-4; the mean germination percentage of three independent KAI2 chimeric variants lines on PAC (20 μM), DMSO (0.1%) or *rac*-GR24 (1 μM). Lane 5-12; Graphic representation of 93 insertion lines. Each blue box represents the amino acid position in KAI2 where a ShHTL7 amino acid is substituted. Lane 13; degree of rescue of the *htl-3* leaf shape phenotype by each KAI2 chimeric variant (**Supplementary Fig 5**). Colors are from 0% rescued (yellow) to 100% rescued (dark green). Grey indicates that the variant was not available. Representative pictures of *htl-3*, *35S::KAI2*, Var19 and Var64 plants. Are shown on the right inserts. **b**. Scatterplot showing the log-fold change scores calculated for each KAI2 chimeric variant with full-length protein, empty vector control and MAX2 fragments using a Y2H protein interaction assay (see **Supplementary Fig. 3**). 22 scores were calculated for each variant. Red dotted line represents four standard deviations from the mean. **c.** SL dose response germination curves**.** Percent germination of mis-expressed *ShHTL7*, *KAI2* and three independent Var64 seed (64A, 64B, 64C) on PAC (20 μM) and increasing *rac*-GR24 concentrations. Four-parameter logistic curves were fitted to the data, and EC_{50} values, ± standard error, of *rac*-GR24 concentrations have been included for those lines showing response to SL. Bases on these curves the effective concentration that germinates 50% of seed EC_{50} was calculated and is shown in the box.

Fig. 2. Conservation of Var64 amino acids in land plants. a. Phylogenetic tree built using *KAI2/DLK/DDK* sequences from across the land plant phylogeny, rooted using *KAI2* sequences from hornworts. Sequences within each of the three coloured clades were investigated in more detail for their similarity with variant 64 at positions 153, 157 and 190**. b**. *KAI2* conserved sequences from angiosperms. **c**. *KAI2* divergent sequences from parasitic Orobanchaceae. Coloured boxes beside the clades indicate amino acid similarity with variant 64 at positions 153

(blue), 157 (green) or 190 (purple). **James, we need a list of what the similar amino acids are for each catagory!**

Figure 3. A. **Var64 responds to both GR24 enantiomers a.** Percent germination of *htl-3*, mis-expressed *KAI2* and three independent Var64 seed lines (64A, 64B, 64C) on PAC (20μM) with DMSO, 1 μM (−)-(2'*S*)-GR24 or (+)-(2'*R*)-GR24. **b**. SL inhibits YLG hydrolysis. Competitive binding assay using YLG and *rac*-GR24 to evaluate the changes in YLG hydrolysis by KAI2 (black) and Var64 (blue) after incubation with 0.5 μM *rac*-GR24. Error bars represent SD values from three independent experiments. **c**. Hydrolysis activity towards GR24 enantiomers. UPLC-UV (260 nm) analysis was used to detect the remaining amount of GR24 isomers. Box plots of n=3 replicates represent the hydrolysis rate calculated from the remaining GR24 isomers and analogs taking into account the hydrolysis in the buffer alone (non protein sample), quantified using indanol as internal standard. Letters indicate different statistical groups (ANOVA, post-hoc Tukey test). **d**. KAR_2 dose response germination curves. Mis-expressed *ShHTL7*, *KAI2* and three independent Var64 seed (64A, 64B, 64C) on PAC (20 μM) and increasing KAR_2 concentrations. Four-parameter logistic curves were fitted to the data, and EC_{50} values, ± standard error, of KAR_2 concentrations have been included for those lines showing response to karrikin. Based on these curves the effective concentration that germinates 50% of seed (EC_{50}) was calculated and is shown in the box. **Alex I need your data to be converted to box plots and I only need the data for GR24. Also I need the stats included in the figure.**

Figure 4. Var64 derived amino acids create a SL binding domain. a. The substitution of KAI2 aromatic residues for ShHTL7 equivalents results in the disruption of several interactions (purple dashed lines) along the X-axis of the protein. This disruption translates into increased motility of the lid domain (Supplemental Movie 1), consistent with the receptor's new ability to accommodate SL molecules. **b.** Pocket alignment of KAI2 and Var64 receptors reveals an 11.5 Å larger pocket mouth (orange shading) and a 29.7% increased pocket volume in the Var64 receptor. The pocket mouths are shown in yellow shading with width shown in $Å^2$. **c.** A summary of the three most common binding states between Var64, KAI2, and *2'R*-GR24. Molecular dynamic simulations of Var64 and KAI2 receptors to determine binding modes of ligand-protein complexes over a 10 ns simulation. Var64-(*2'R*)-GR24 complex was found in a

productive binding mode 47.8% of the time whist the same state was only found 2.1% of the time for the KAI2 complex. **d.** Calculation of the magnitude change in the pose of the ligand throughout the MD simulation. Both proteins stabilized the ligand after 1 ns of simulation, but its position on the KAI2 pocket is compromised from the 4 ns mark as the interaction is not strong nor stable.

Figure 1

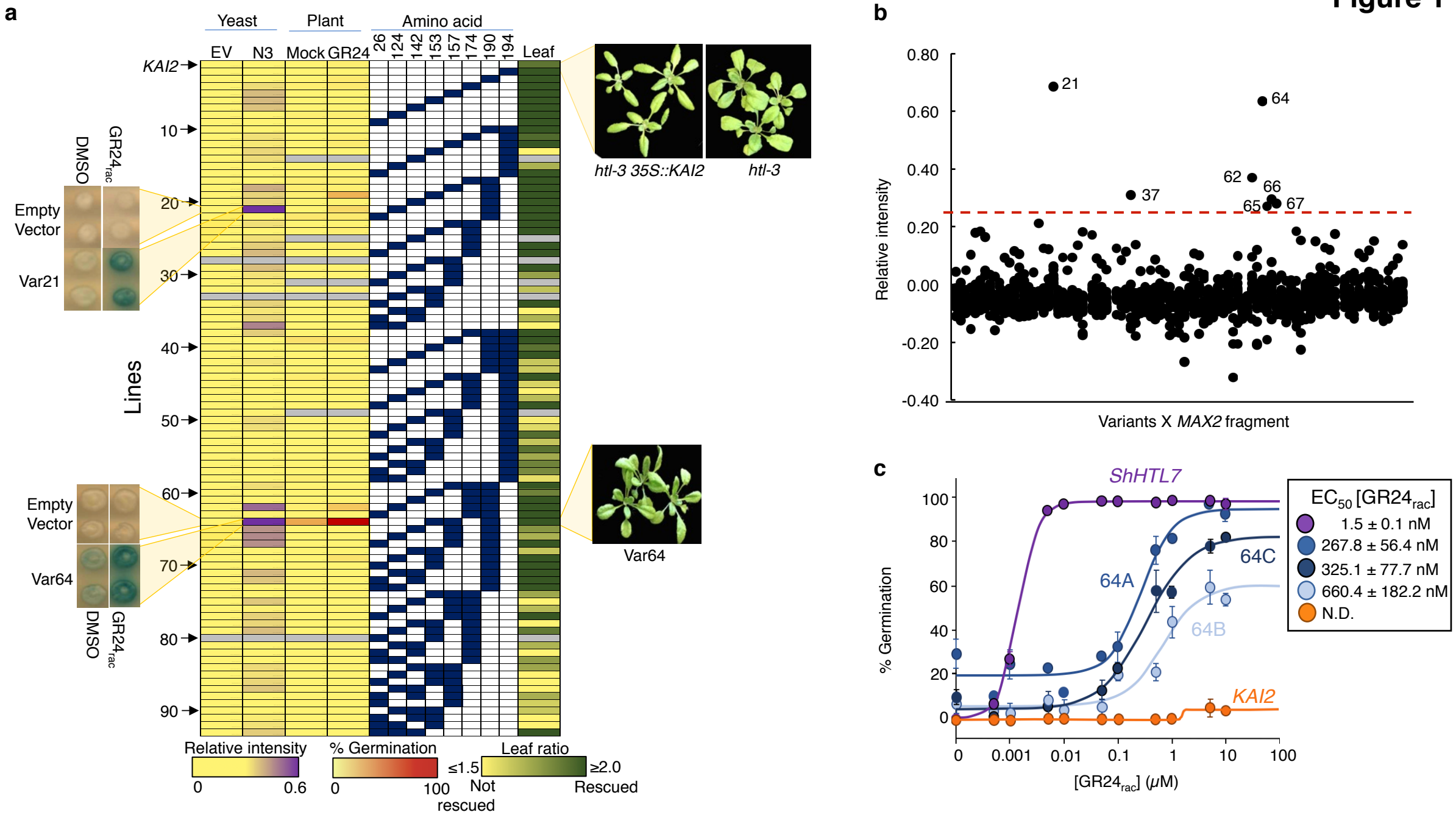
a
Yeast
Plant
Amino acid
EV
N3
Mock
GR24
26
124
142
153
157
174
190
194
Leaf
KAI2
10
20
30
40
50
60
70
80
90
Lines
DMSO
GR24rac
Empty Vector
Var21
Empty Vector
Var64
DMSO
GR24rac
htl-3 35S::KAI2
htl-3
Var64
Relative intensity
0
0.6
% Germination
0
100
≤1.5
Not rescued
Leaf ratio
≥2.0
Rescued
b
0.80
0.60
0.40
0.20
0.00
-0.20
-0.40
Relative intensity
21
64
62
66
37
65
67
Variants X MAX2 fragment
c
ShHTL7
64C
64A
64B
KAI2
100
80
60
40
20
0
% Germination
0
0.001
0.01
0.1
1
10
100
[GR24rac] (μM)
EC50 [GR24rac]
1.5 ± 0.1 nM
267.8 ± 56.4 nM
325.1 ± 77.7 nM
660.4 ± 182.2 nM
N.D.

Figure 2

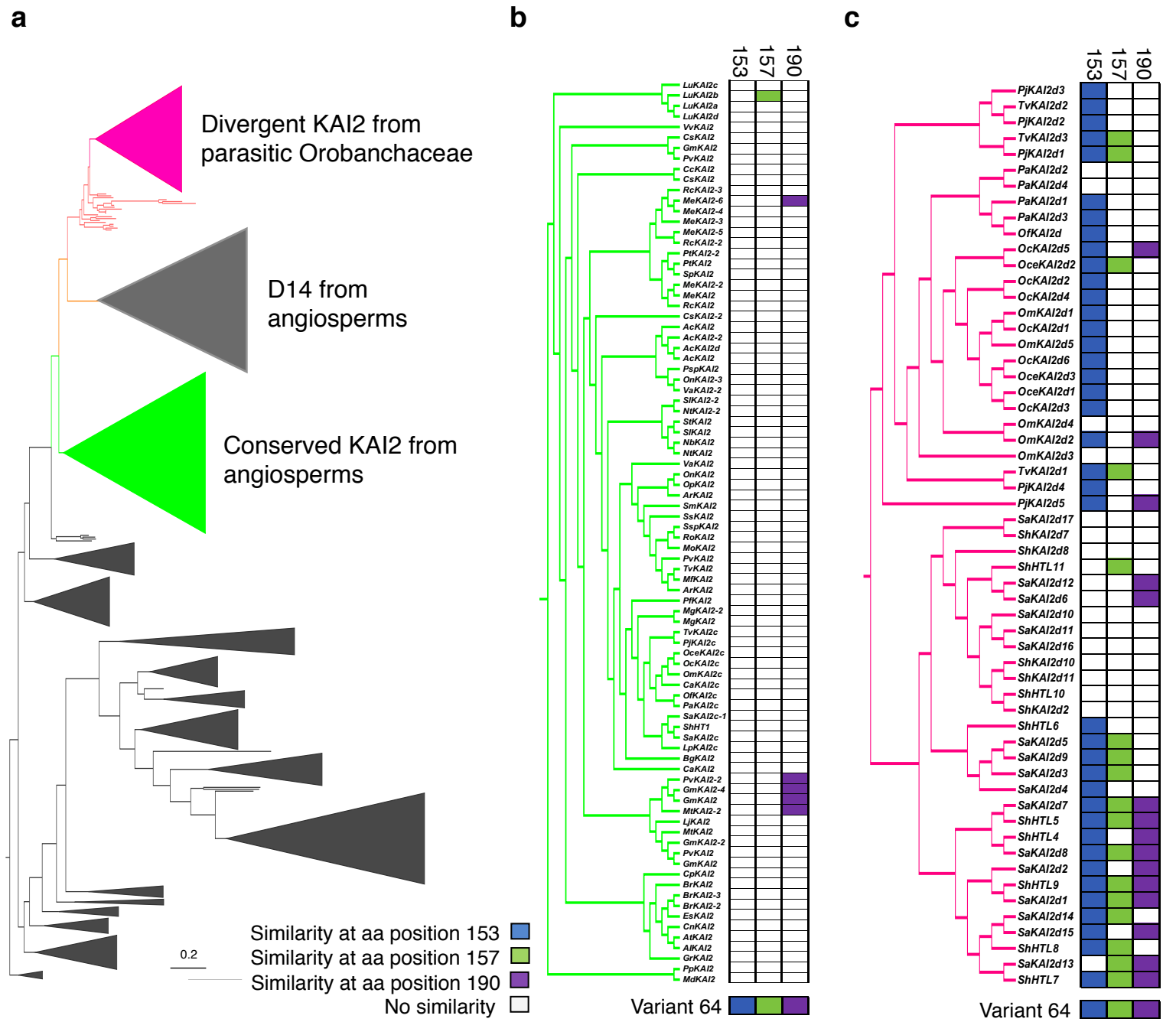
a
b
c
Divergent KAI2 from parasitic Orobanchaceae
D14 from angiosperms
Conserved KAI2 from angiosperms
0.2
Similarity at aa position 153
Similarity at aa position 157
Similarity at aa position 190
No similarity
153
157
190
Variant 64
LuKAI2c
LuKAI2b
LuKAI2a
LuKAI2d
VvKAI2
CsKAI2
GmKAI2
PvKAI2
CcKAI2
CsKAI2
RcKAI2-3
MeKAI2-6
MeKAI2-4
MeKAI2-3
MeKAI2-5
RcKAI2-2
PtKAI2-2
PtKAI2
SpKAI2
MeKAI2-2
MeKAI2
RcKAI2
CsKAI2-2
AcKAI2
AcKAI2-2
AcKAI2d
AcKAI2
PspKAI2
OnKAI2-3
VaKAI2-2
SlKAI2-2
NtKAI2-2
StKAI2
SlKAI2
NbKAI2
NtKAI2
VaKAI2
OnKAI2
OpKAI2
ArKAI2
SmKAI2
SsKAI2
SspKAI2
RoKAI2
MoKAI2
PvKAI2
TvKAI2
MfKAI2
ArKAI2
PfKAI2
MgKAI2-2
MgKAI2
TvKAI2c
PjKAI2c
OceKAI2c
OcKAI2c
OmKAI2c
CaKAI2c
OfKAI2c
PaKAI2c
SaKAI2c-1
ShHT1
SaKAI2c
LpKAI2c
BgKAI2
CaKAI2
PvKAI2-2
GmKAI2-4
GmKAI2
MtKAI2-2
LjKAI2
MtKAI2
GmKAI2-2
PvKAI2
GmKAI2
CpKAI2
BrKAI2
BrKAI2-3
BrKAI2-2
EsKAI2
CnKAI2
AtKAI2
AlKAI2
GrKAI2
PpKAI2
MdKAI2
PjKAI2d3
TvKAI2d2
PjKAI2d2
TvKAI2d3
PjKAI2d1
PaKAI2d2
PaKAI2d4
PaKAI2d1
PaKAI2d3
OfKAI2d
OcKAI2d5
OceKAI2d2
OcKAI2d2
OcKAI2d4
OmKAI2d1
OcKAI2d1
OmKAI2d5
OcKAI2d6
OceKAI2d3
OceKAI2d1
OcKAI2d3
OmKAI2d4
OmKAI2d2
OmKAI2d3
TvKAI2d1
PjKAI2d4
PjKAI2d5
SaKAI2d17
ShKAI2d7
ShKAI2d8
ShHTL11
SaKAI2d12
SaKAI2d6
SaKAI2d10
SaKAI2d11
SaKAI2d16
ShKAI2d10
ShKAI2d11
ShHTL10
ShKAI2d2
ShHTL6
SaKAI2d5
SaKAI2d9
SaKAI2d3
SaKAI2d4
SaKAI2d7
ShHTL5
ShHTL4
SaKAI2d8
SaKAI2d2
ShHTL9
SaKAI2d1
SaKAI2d14
SaKAI2d15
ShHTL8
SaKAI2d13
ShHTL7

Figure 3

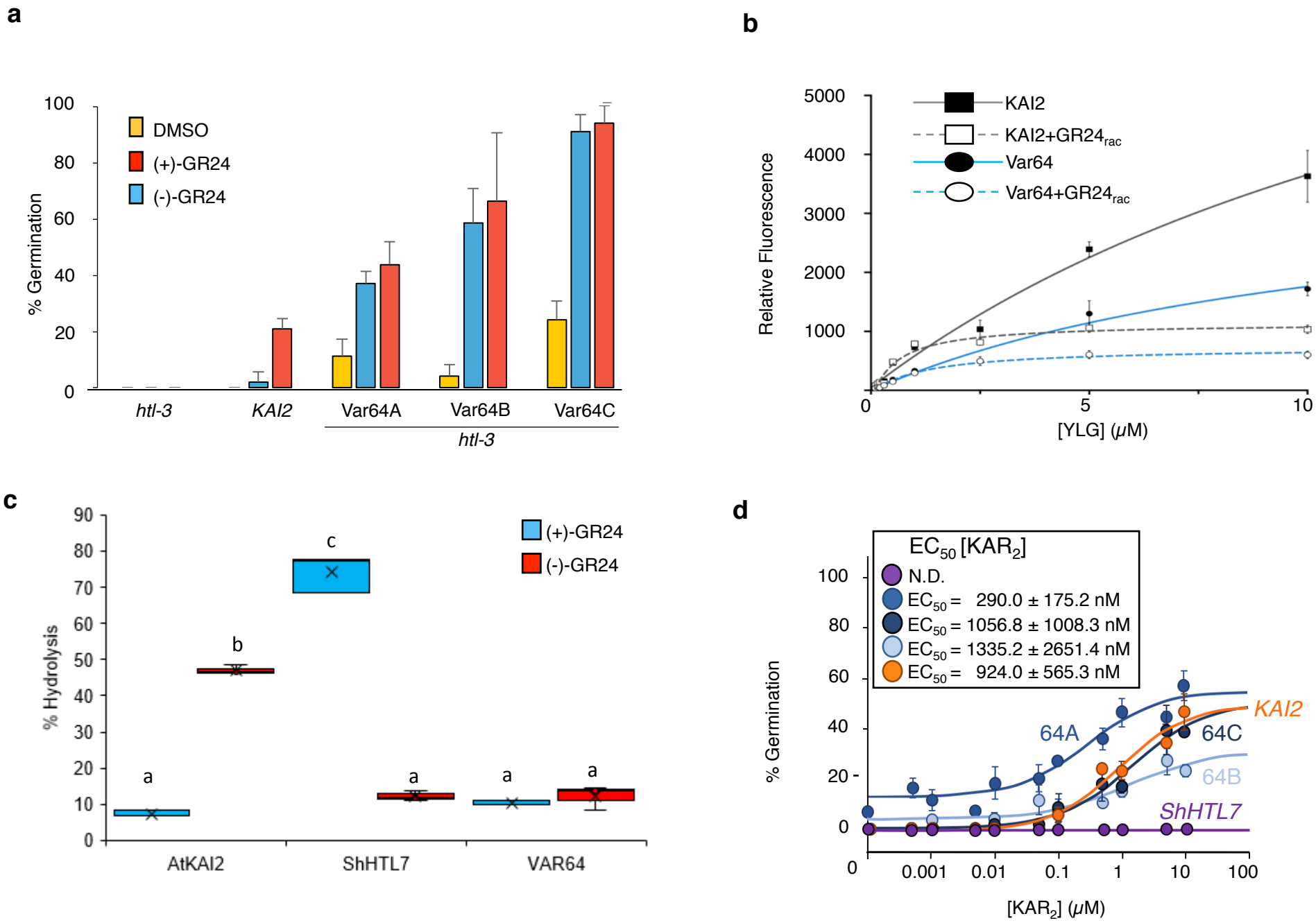
a
100
80
60
40
20
0
% Germination
DMSO
(+)-GR24
(-)-GR24
htl-3
KAI2
Var64A
Var64B
Var64C
htl-3
b
5000
4000
3000
2000
1000
0
Relative Fluorescence
KAI2
KAI2+GR24rac
Var64
Var64+GR24rac
0
5
10
[YLG] (μM)
c
90
80
70
60
50
40
30
20
10
0
% Hydrolysis
(+)-GR24
(-)-GR24
a
b
c
a
a
a
AtKAI2
ShHTL7
VAR64
d
EC50 [KAR2]
N.D.
EC50 = 290.0 ± 175.2 nM
EC50 = 1056.8 ± 1008.3 nM
EC50 = 1335.2 ± 2651.4 nM
EC50 = 924.0 ± 565.3 nM
100
80
60
40
20
0
% Germination
64A
64C
KAI2
64B
ShHTL7
0
0.001
0.01
0.1
1
10
100
[KAR2] (μM)

Figure 4

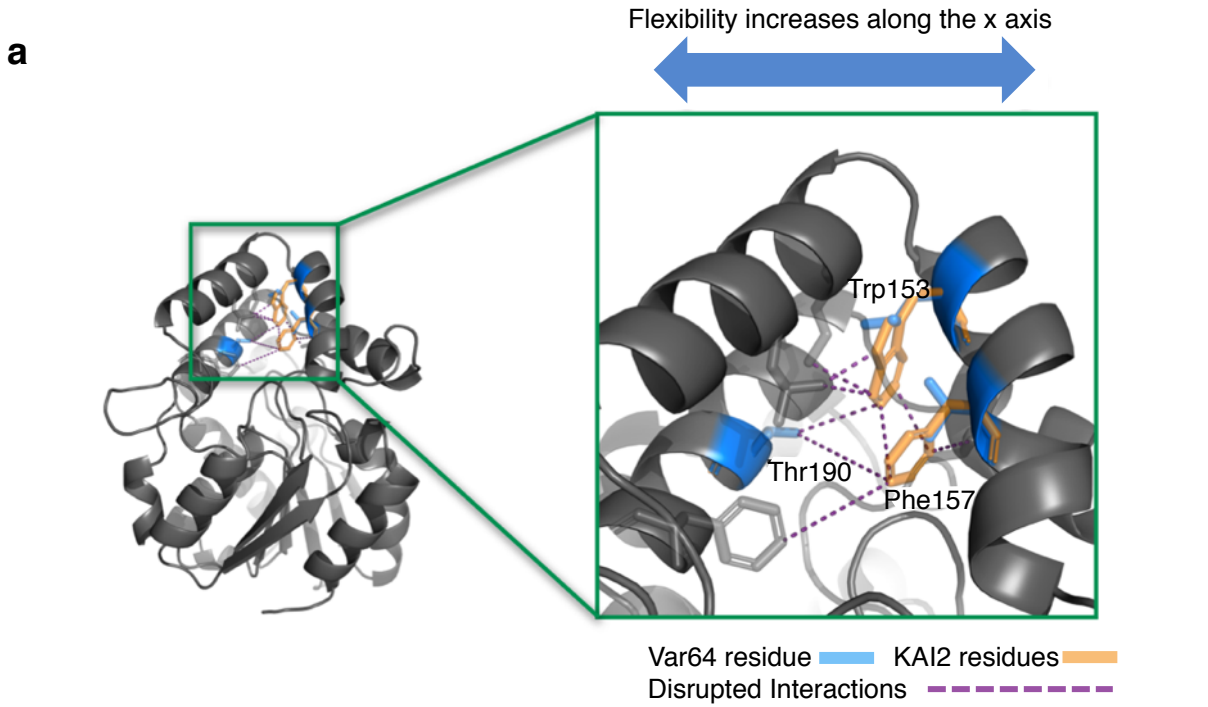
a
Flexibility increases along the x axis
Trp153
Thr190
Phe157
Var64 residue
KAI2 residues
Disrupted Interactions

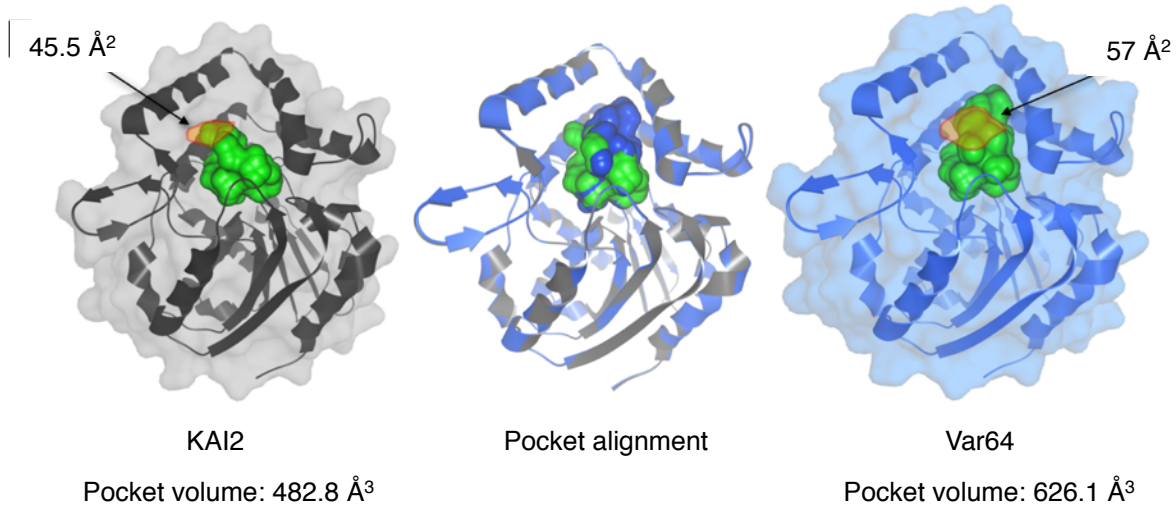
b
45.5 Å²
57 Å²
KAI2
Pocket alignment
Var64
Pocket volume: 482.8 Å³
Pocket volume: 626.1 Å³

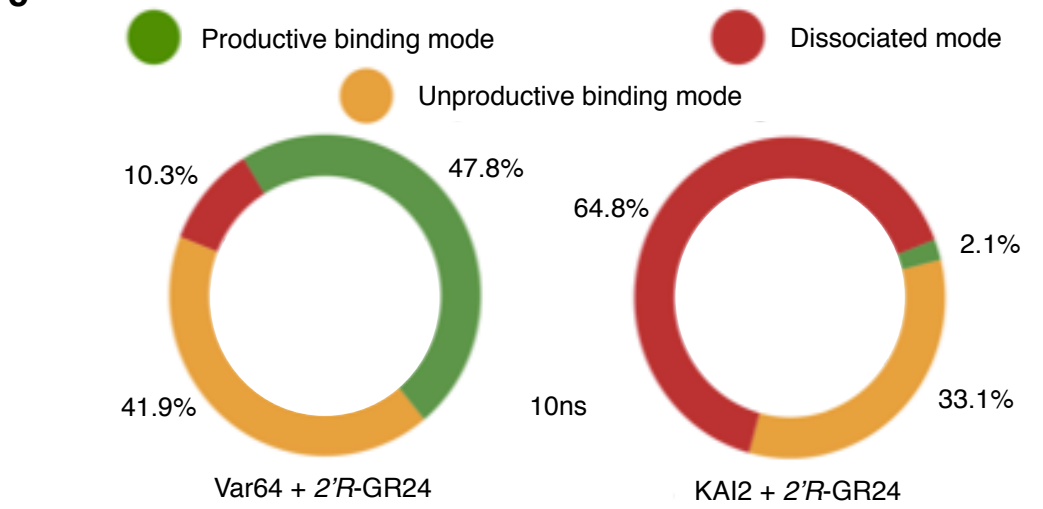
c
Productive binding mode
Dissociated mode
Unproductive binding mode
10.3%
47.8%
41.9%
Var64 + 2'R-GR24
64.8%
2.1%
10ns
33.1%
KAI2 + 2'R-GR24

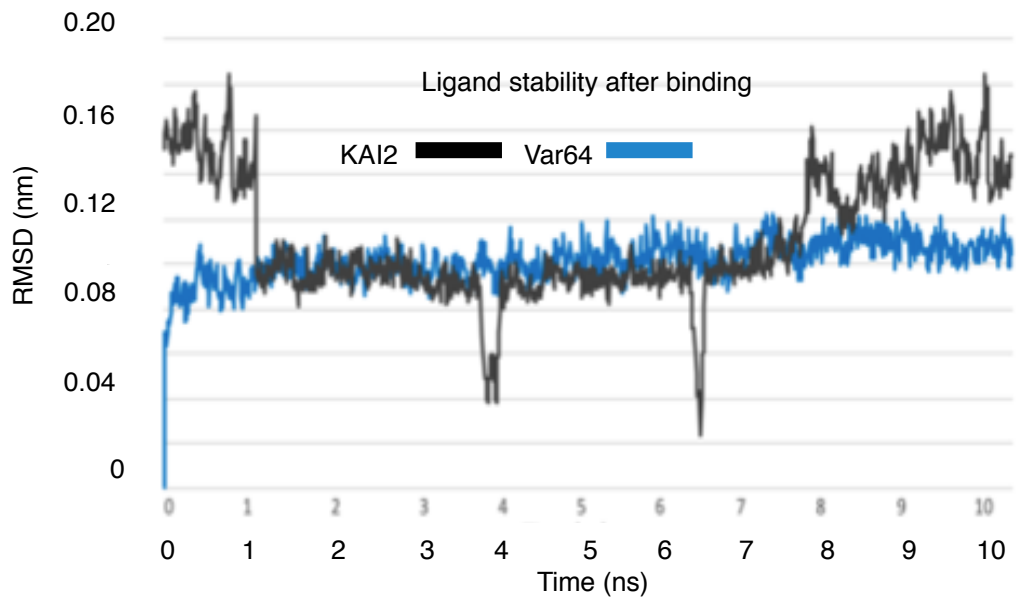
d
Ligand stability after binding
KAI2
Var64
RMSD (nm)
0.20
0.16
0.12
0.08
0.04
0
0 1 2 3 4 5 6 7 8 9 10
Time (ns)

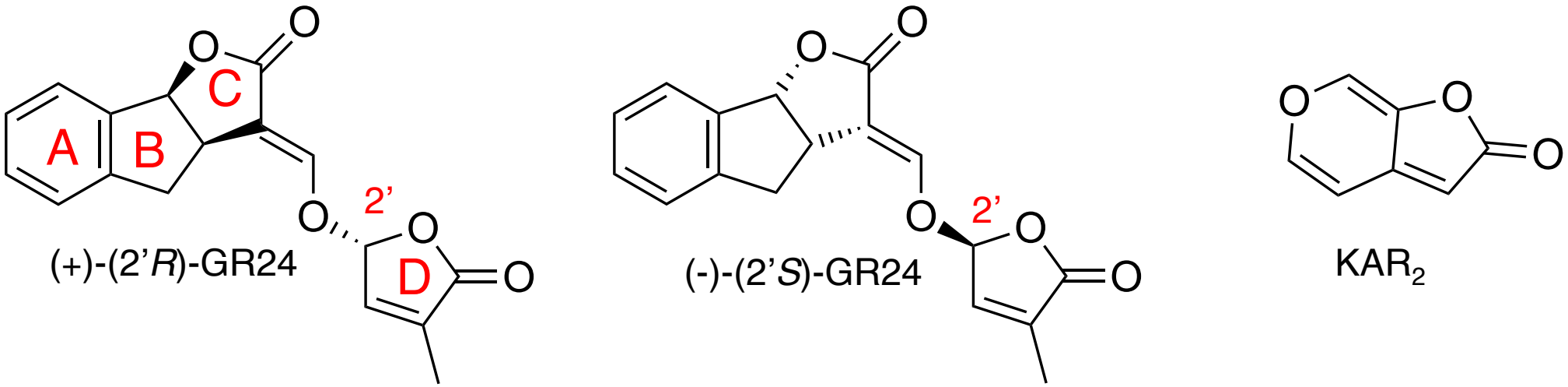

Supplementary Fig. 1. Structures of 2'*R*- and 2'*S*-enantiomeric forms of strigolactones (SLs) and karrikin (KAR_2). For SLs the synthetic GR24 is shown and the 2' chirality is at the enol-ether bridge between the C and D-ring. For karrikin KAR_2 is shown.

a

Residue	KAI2	ShHTL7
26	Phe	Tyr
95	Ser	Ser
121	Ser	Thr
124	Tyr	Leu
134	Phe	Phe
139	Leu	Met
142	Leu	Thr
143	Phe	Leu
146	Ile	Leu
153	Trp	Leu
154	Cys	Ser
157	Phe	Thr
161	Ala	Leu
174	Phe	Tyr
190	Gly	Thr
193	Ile	Ile
194	Phe	Cys
196	Ser	Leu
217	Asp	Asp
219	Ala	Met
246	His	His

b

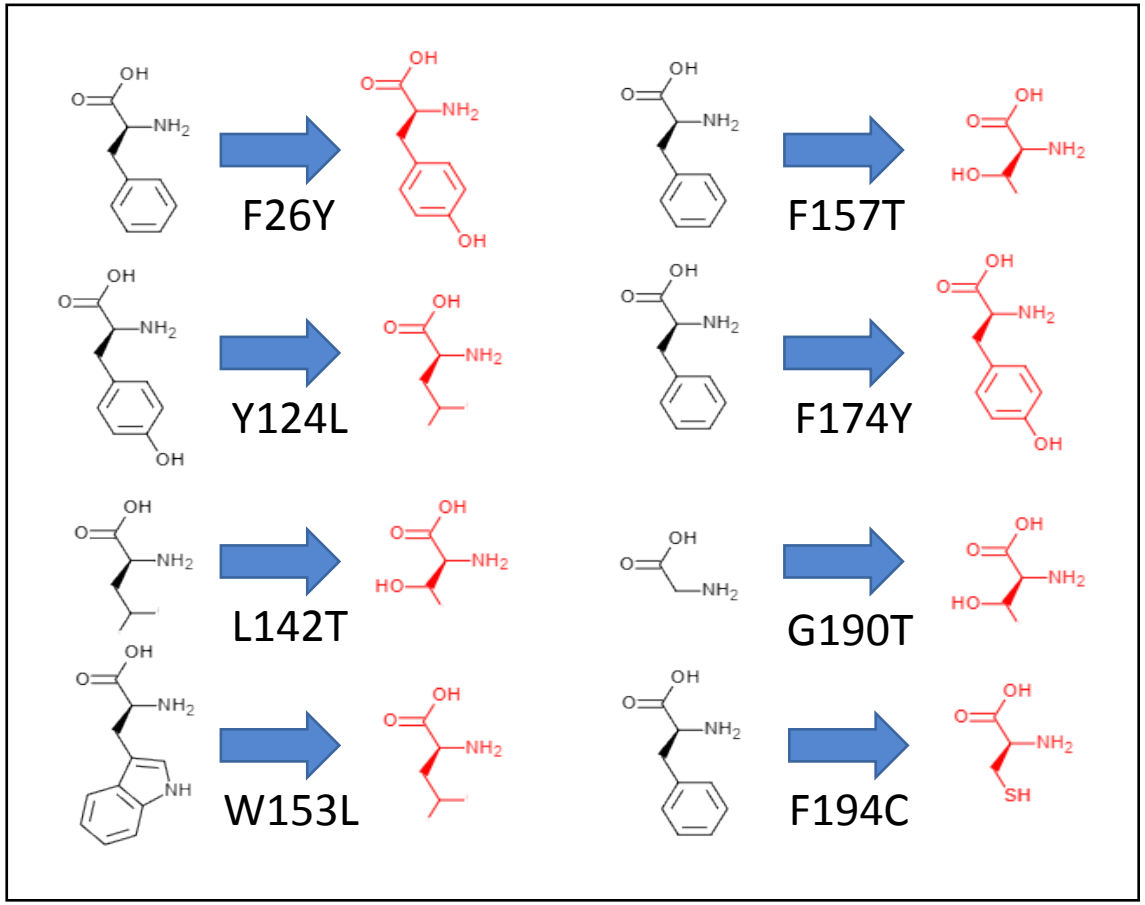

c

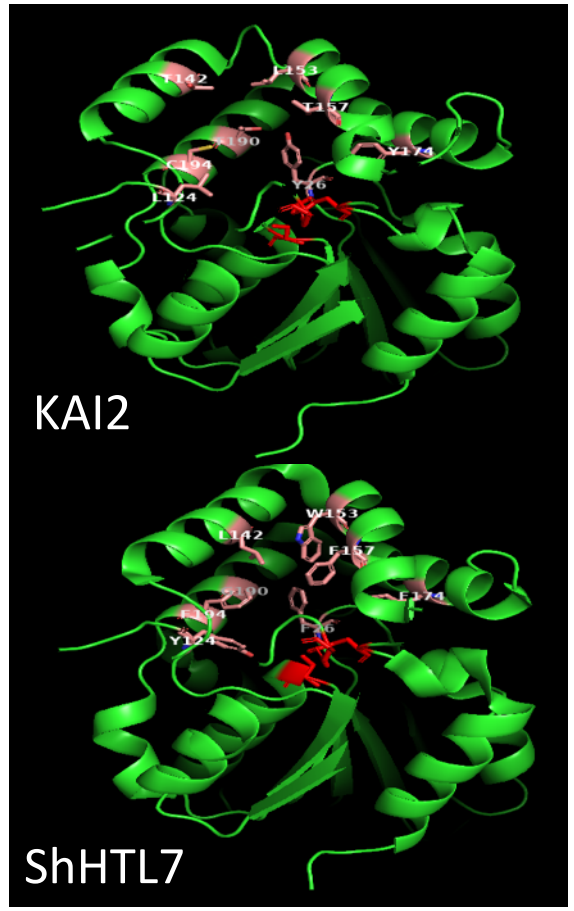

Catalytic triad
Polar side chain
Non Polar side chain
Electrically charged side chain

Supplementary Fig. 2 Selection of ShHTL7 residues for substitution in KAI2. a. The choice of the eight substitutions (pink boxes) were made based on increased polarity and decreased size (blue amino acids) in ShHTL7 versus the KAI2 equivalent. Red boxes represent the three catalytic residues. **b.** Chemical structures of the amino acids at the positions substituted in KAI2 to generate JGI variants. Structures in black represent the amino acids present at these positions in KAI2, structures in red represent their counterparts in ShHTL7. Letter codes and numbers below the arrows denote the substitutions that were made to produce the JGI variants **c.** Crystal models representing the eight residues highlighted in pink, The three catalytic residues highlighted in red, Structures are visualized using PYMOL version 2.3.2.

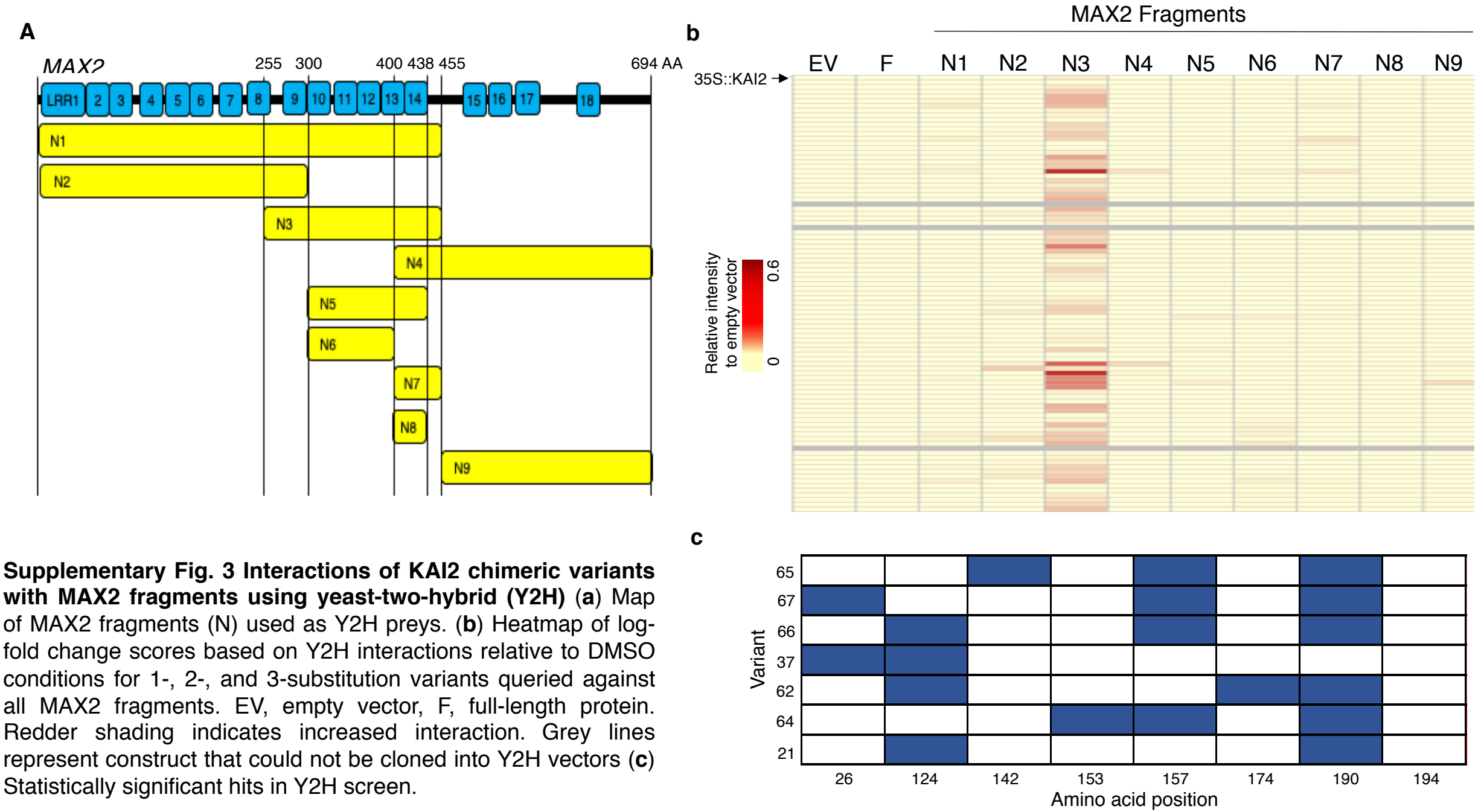

Supplementary Fig. 3 Interactions of KAI2 chimeric variants with MAX2 fragments using yeast-two-hybrid (Y2H) (**a**) Map of MAX2 fragments (N) used as Y2H preys. (**b**) Heatmap of log-fold change scores based on Y2H interactions relative to DMSO conditions for 1-, 2-, and 3-substitution variants queried against all MAX2 fragments. EV, empty vector, F, full-length protein. Redder shading indicates increased interaction. Grey lines represent construct that could not be cloned into Y2H vectors (**c**) Statistically significant hits in Y2H screen.

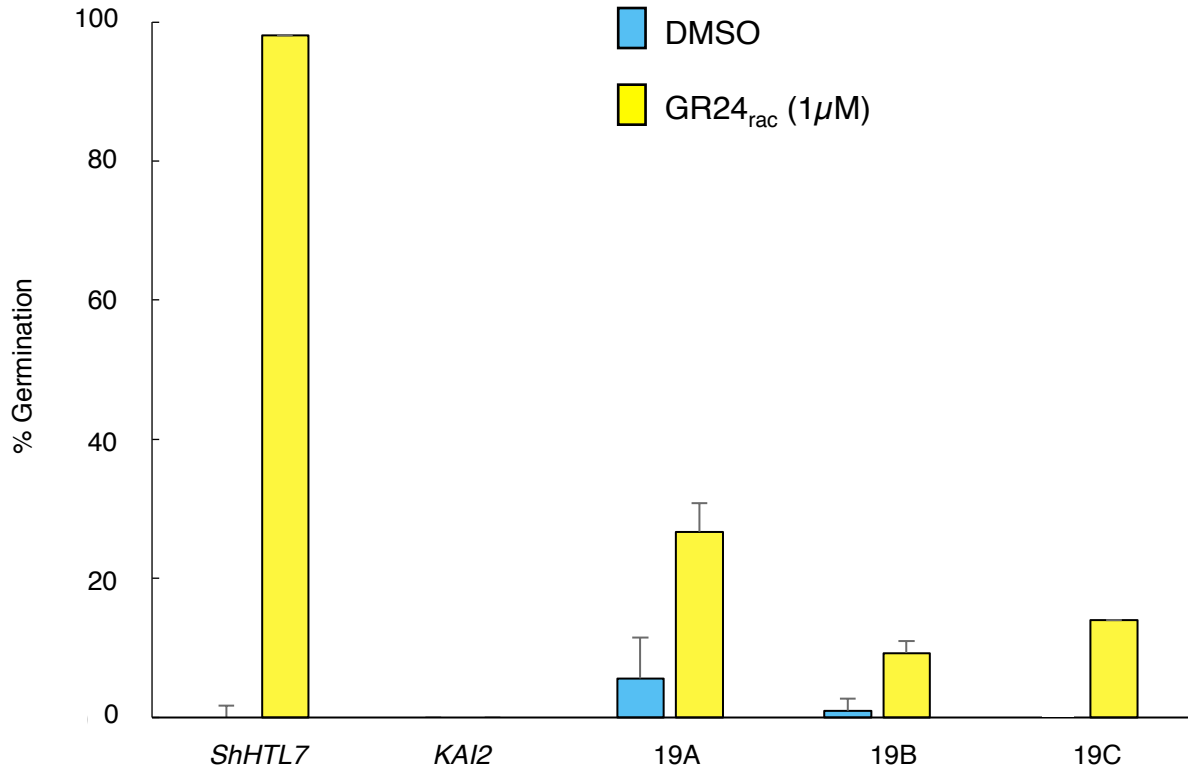

Supplementary Fig. 4 Var19 germination on SL. Mis-expressed *ShHTL7*, *KAI2* and three independent Var19 lines (19A, 19B, 19C) on PAC (20μM) plus or minus $Gr24_{rac}$ concentrations. Each line was tested three times Bar = S.D

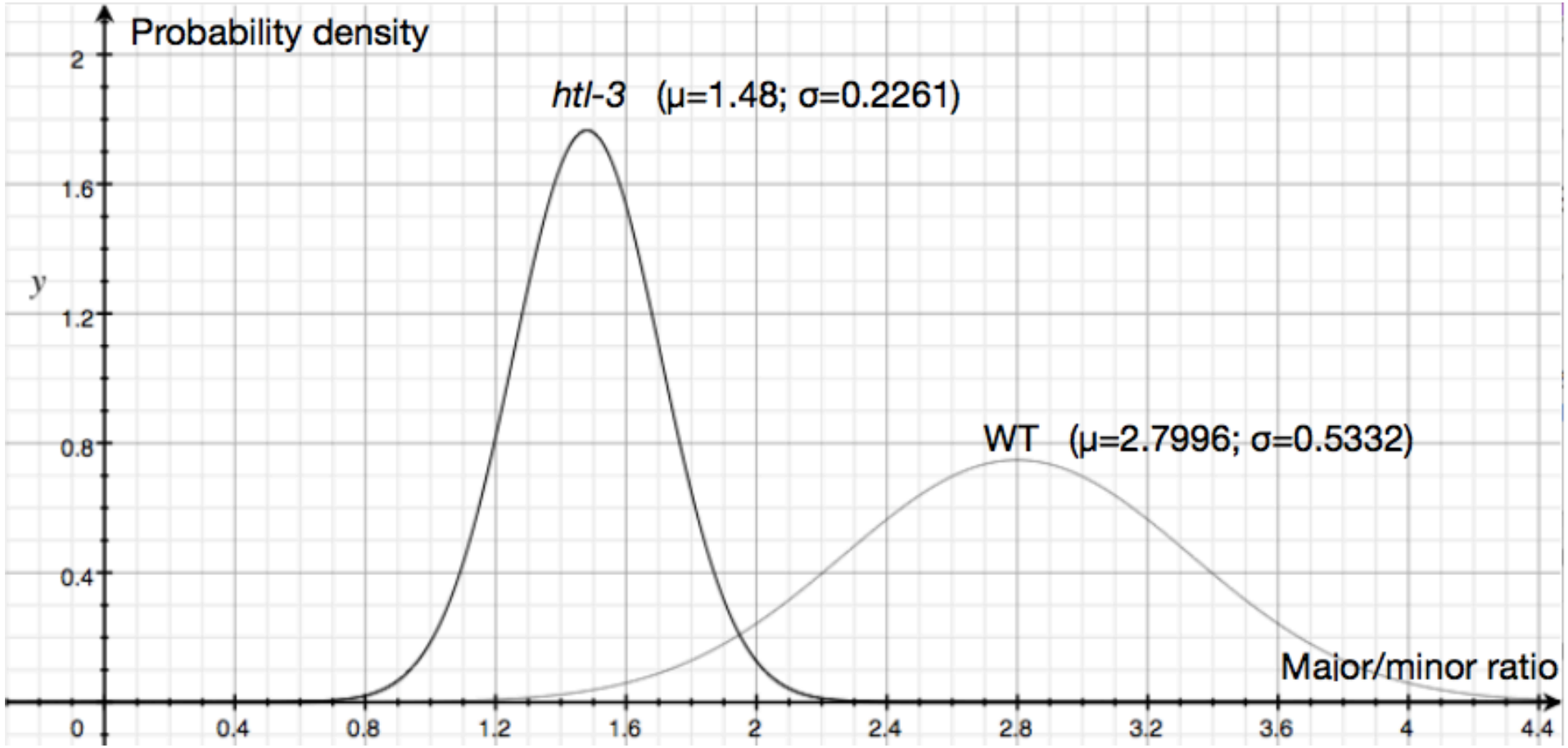

Supplementary Fig. 5 Standard distribution of length/width (major/minor) ratio *of htl-3* and wild type Columbia (WT) leaves. Each distribution was a normal distribution based on the population mean (μ) and standard deviation (σ) approximated by that of the 26 control samples. WT: y=(1/(0.53332•√(2π)))•*e*-(x-2.7996)^2/(2•(0.53332)^2); *htl-3*: y=(1/(0.2261•√(2π)))•*e*-(x-1.48)^2/(2•(0.2261)^2). Three categories given by 5% cutoff: *htl-3*: x<1.85; WT: x>1.92; ambiguous: 1.85<x<1.92. Based on the two distributions, in order to meet the 0.05 significance level, any sample data smaller than 1.85 would be considered as *htl-3*, while sample data larger than 1.92 would be considered as wild type. Note that there is an ambiguous region in between (1.82-1.92) where the phenotype can not be statistically determined in this case.